Kinetic resonances and stratification of the positive column of a discharge

Yu. B. Golubovskii and A. Yu. Skoblo*
Institute of Physics, Saint-Petersburg State University, ul. Ulianovskaja 1, 198504 Saint-Petersburg, Russia

C. Wilke, R. V. Kozakov, and J. Behnke
Institute of Physics, University of Greifswald, Domstrasse 10a, 17489 Greifswald, Germany

V. O. Nekutchaev
Ukhta Industrial State University, ul. Senjukova 13, 163700 Ukhta, Russia
(Received 20 May 2005; published 29 August 2005)

Resonance formation of the electron velocity distribution function (EDF) in an inert gas dc discharge at low pressures and small currents is analyzed on the basis of an accurate numerical solution of the Boltzmann kinetic equation in spatially periodic sinusoidally modulated striation-like fields. Calculations are performed for neon at pressures around 1 Torr. The dependences of the EDF, electron density and mean energy, and excitation rate on the electric field spatial period length are investigated. In addition to resonances corresponding to *S* and *P* striations predicted by linear analytical theory, the kinetic model indicates the presence of a resonance that can be attributed to an *R* striation. This resonance is more pronounced at lower pressures when *R* striations are observed experimentally. The influence of inelastic collisions on the EDF formation in the resonance fields is analyzed.

DOI: 10.1103/PhysRevE.72.026414 PACS number(s): 52.25.Dg, 52.35.Mw, 52.80.Hc

I. INTRODUCTION

The positive column of an inert gas dc glow discharge is stratified over a wide range of discharge conditions, i.e., exists in a regime of propagation of ionization waves (striations) where all internal plasma parameters vary periodically in space and time. By the end of the 1960s striations were understood as waves of an ionization-diffusion nature as discussed in detail in reviews [1–3]. The plasma was described by a system of hydrodynamic equations including continuity equations for charged particles and metastable atoms, electron momentum, and energy balance equations. The origin and propagation of striations was considered as a development of instabilities. The qualitative picture of discharge stratification is given from this point of view in [4]. The hydrodynamic approach is applicable if the electron velocity distribution function (EDF) is formed locally due to electron-atom and electron-electron collisions in each striation phase as a function of the electric field. Therefore the range of applicability of this approach is limited to sufficiently high pressures and(or) large discharge currents.

At low pressures (units of Torr) and small currents (tens of mA) the electron distribution function is formed by the whole potential profile of the striation rather than by the local field. In this case, the electron motion should be treated from the nonlocal kinetics point of view. Since the 1970s investigations of the EDF in spatially periodic striationlike electric fields on the basis of the Boltzmann kinetic equation solution with the spatial gradients being taken into account [5] have been published.

Tsendin [6] developed an approach to the mechanism of an inert gas discharge stratification basing on nonlocal electron kinetics in spatially periodic electric fields. At low pressures and small currents the electron energy balance is controlled mainly by inelastic collisions with atoms. Electrons are accelerated by the action of electric field, with their total energy $\varepsilon = U + e\varphi$ (U and $e\varphi$ are the kinetic and potential energy of an electron with the charge $e = -e_0$, φ is the potential) being approximately constant. A small decrease of ε is caused by the small loss of electron energy in elastic collisions with atoms. When the electron kinetic energy attains the atom excitation threshold U_1, electrons can undergo inelastic impacts. After a loss of energy equal to U_1 they are accelerated again, and the process is repeated. The EDF and the spatially periodic field with a spatial period length L_S (striation length) are formed in a self-consistent way. The mechanism described above determines the spatial and energy periods. The fall of the potential over a striation length $V_L^{(S)}$ is determined by the energy period equal to the sum of the energy loss in inelastic collisions U_1 and the small energy loss in elastic collisions ΔU: $e_0 V_L^{(S)} = U_1 + \Delta U$. The spatial period length equals $L_S = V_L^{(S)}/E_0$, here E_0 is the period-averaged axial electric field. It was shown in [6] that the presence of elastic collisions results in an electron bunching effect that consists of compressing the EDF to a narrow maximum moving in a plane (total energy ε, axial coordinate z) along the resonance trajectory which is close to a straight line parallel to the z axis (it corresponds to conservation of the total energy). Formation of the EDF structure in the spatially periodic fields has an explicit resonance character. If the field spatial period length L differs from the resonance length L_S (small detuning from resonance) destruction of the EDF structure takes place. The linear analytical theory [6,7] predicts kinetic resonances not only at the period length $L = L_S$ but also at lengths $L = L_S$, $L_S/2$, $L_S/3$, etc., that correspond to higher harmonics. The EDF in the resonance fields

*Electronic address: alexey_skoblo@yahoo.com

(i.e., with the field's spatial period length being equal to $L=L_S, L_S/2, L_S/3, \ldots$) has the form of maxima moving in the plane (energy, coordinate) along the resonance trajectories. At $L=L_S/2, L_S/3, \ldots$ the number of EDF peaks and resonance trajectories equals 2,3,… correspondingly.

Spatial relaxation of the EDF in the uniform and striation-like spatially periodic fields was analyzed in [8,9] on the basis of the accurate numerical solution of the Boltzmann kinetic equation taking elastic and conservative inelastic collisions with atoms into account. The EDF relaxation in the spatially periodic field leads to the bunching of the EDF. Electron energy losses in elastic impacts as well as the presence of several excited atomic states were demonstrated in [9] to lead to the EDF bunching. Similar results were obtained in [10] based on an analytical solution of the Boltzmann equation. The EDFs formed in the resonance fields and also in the fields with the deviations of the spatial period towards smaller or larger values were discussed in [11,12] together with the resonance behavior of the macroscopic quantities (electron density and mean energy).

There are three different types of the self-excited ionization waves (*S*, *P*, and *R* striations) in an inert gas dc glow discharge at low pressures and small currents that can be observed in experiment [1,13]. These types of striations differ by the magnitudes of frequency ν, wavelength (striation length) L, and potential drop on the wavelength $V_L=E_0L$. In an *S* striation the fall of the potential V_L slightly exceeds an atom excitation threshold. Particularly, for neon $V_L \approx (17-22)$ V under different discharge conditions. Therefore in an *S* striation the potential drop V_L corresponds to the value $e_0V_L^{(S)}=U_1+\Delta U$ (for neon $U_1=16.6$ eV) and the striation length equals the resonance length $L_S=V_L^{(S)}/E_0$. Hence the kinetic resonance at $L=L_S$ corresponds to an *S* striation [6,7,9,12,14]. For this reason the notations $V_L^{(S)}$ and L_S were used above. In a *P* striation the potential drop on the striation length V_L and the striation length L are approximately two times smaller than those in an *S* striation. *P* striations correspond to resonance at $L=L_P=L_S/2$ [7,9,12,14]. Comparison of the experimentally measured EDFs in *S* and *P* striations [12,14] with the calculated electron distribution functions [9,12,15] shows a good agreement between the theory and experiment. The self-excited striations corresponding to higher harmonics (e.g., for $L=L_S/3$) have not been observed experimentally.

Experimental values of the potential drop V_L and striation length L in an *R* striation are intermediate between the corresponding values in *S* and *P* striations. Particularly for neon, in an *R* striation $V_L \approx (12-14)$ V. The linear theory [6,7] based on an approximate analytical solution of the kinetic equation in spatially periodic weakly modulated fields did not predict a resonance that could be attributed to an *R* striation.

In the present paper, the resonance behavior of the EDF is studied based on an accurate numerical solution of the Boltzmann kinetic equation in sinusoidally modulated striation-like fields with a large modulation degree for different spatial period lengths in the range $L_S/3$ to L_S. It is shown that in addition to resonances corresponding to *S* and *P* striations, the resonance that can be connected with an *R* striation takes place. The measurements of the frequency, wavelength, and potential drop over the wavelength were performed at low pressures and small currents for different values of the discharge current to illustrate the existence ranges of various types of striations.

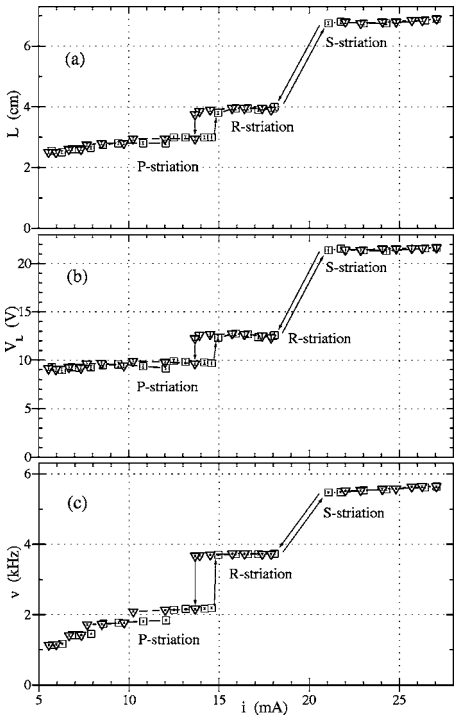

FIG. 1. Experimental dependences of the wavelength L (a), fall of the potential over the wave length V_L (b), and frequency ν (c) on the discharge current for the self-excited striations in neon at pressure $p=1.5$ Torr. The dependences for increasing (squares) and decreasing (triangles) current.

II. MEASUREMENTS OF THE STRIATION PARAMETERS IN NEON DISCHARGE AT LOW PRESSURES AND SMALL CURRENTS

The measurements of the striation parameters were performed in a dc discharge in neon at pressure $p=1.5$ Torr, tube radius $R_0=1$ cm, and current $i<(25-30)$ mA. The discharge current i was stabilized by the current source based on a high voltage field-controlled transistor. Two photodiodes were used to visually analyze the oscillations of the plasma radiation intensity, and measure the frequency ν and wavelength L. The signals produced by the photodiodes positioned near the discharge tube were analyzed by a two channel oscilloscope. The electrostatic voltmeter was used to measure the difference of the mean floating potentials of the two probes and hence the mean axial electric field.

The experimental dependences of the striation parameters such as the wavelength $L(i)$, frequency $\nu(i)$, and potential drop on the wavelength $V_L(i)$, on the discharge current i are represented in Figs. 1(a)–1(c). *P*, *R*, and *S* striations are observed successively with an increase of the current. These three types differ by the values of the potential drop V_L, as demonstrated in Fig. 1(b). The jumps of the striation param-

eters occur with the transitions from one type to another. Hysteresis takes place. The period-averaged axial electric field E_0 weakly depends (decreases) on current, hence the dependences $V_L(i)$ and $L(i)$ have the similar form. The potential drop and wavelength in S striation are $V_L \approx (21-22)$ V and $L \approx (6-7)$ cm; in P striation they are approximately two times smaller: $V_L \approx (9-10)$ V and $L \approx (2.5-3)$ cm; in R striation these quantities have intermediate values: $V_L \approx (12-13)$ V and $L \approx (3.5-4)$ cm.

III. SOLUTION OF THE BOLTZMANN KINETIC EQUATION IN STRIATIONLIKE FIELDS

Resonance behavior of the EDF in the spatially periodic sinusoidally modulated striationlike fields is analyzed on the basis of accurate numerical solution of the one-dimensional Boltzmann equation taking axial coordinate gradients into account. The EDF is assumed to be weakly anisotropic:

$$f\left(v,\frac{v_z}{v},z\right)=\frac{1}{2\pi}\left(\frac{m_e}{2}\right)^{3/2}\left(f_0(U,z)+\frac{v_z}{v}f_1(U,z)\right), \quad (1)$$

here $U=m_e v^2/2$ is the electron kinetic energy, m_e is the electron mass, f_0 is the isotropic part of the EDF, and f_1 is the anisotropic part.

Using the total energy $\varepsilon=U+e\varphi(z)$ and the axial coordinate z as independent variables, the kinetic equation for the isotropic part of the EDF (with the elastic and conservative inelastic electron-atom collisions being taken into account) can be written in the form

$$\frac{\partial}{\partial z}\left(\frac{U}{3NQ_\Sigma(U)}\frac{\partial f_0(\varepsilon,z)}{\partial z}\right)+\frac{\partial}{\partial \varepsilon}\left(\frac{2m_e}{M}U^2NQ^{\mathrm{el}}(U)f_0(\varepsilon,z)\right)$$
$$=\sum_k UNQ_k^{\mathrm{in}}(U)f_0(\varepsilon,z)-\sum_k (U+U_k)NQ_k^{\mathrm{in}}(U+U_k)$$
$$\times f_0(\varepsilon+U_k,z). \quad (2)$$

Here, N is the density of atoms, Q^{el} is the transport cross section of elastic collisions, Q_k^{in} is the cross section of the kth atomic state excitation, U_k is the excitation energy of the kth state, $Q_\Sigma=Q^{\mathrm{el}}+\Sigma_k Q_k^{\mathrm{in}}$ is the total cross section, and M is the atom mass. The kinetic energy U in Eq. (2) is a function of ε and z. The steady-state approximation is used (the time dependence is neglected). It is applicable since the time for establishment of the function f_0 is defined by the frequency of the energy exchange between atoms and electrons and it is much smaller than typical values of the temporal period of striations.

The sinusoidally modulated electric field under consideration has the form

$$E(z)=E_0\left(1+\alpha\sin\frac{2\pi z}{L}\right). \quad (3)$$

Equation (2) is of parabolic type. The boundary conditions are

$$f_0(\varepsilon,z)|_{z=0}=f_0^{\mathrm{init}}(\varepsilon), \quad (4a)$$

$$\left.\frac{\partial f_0(\varepsilon,z)}{\partial z}\right|_{U=0}=0, \quad (4b)$$

$$f_0(\varepsilon,z)|_{U\to\infty}=0. \quad (4c)$$

The solution technique for Eq. (2) with the boundary conditions (4) is analogous to [8,16]. It consists of the injection of an arbitrary function $f_0^{\mathrm{init}}(\varepsilon)$ into the field (3) and subsequently obtaining the spatially periodic established solution [independent of the form of $f_0^{\mathrm{init}}(\varepsilon)$] at sufficiently large distance along z. The cross sections Q^{el} and Q_k^{in} used in the calculations are given in [9]. The normalization factor for the EDF is chosen so that the electron density averaged over a period is equal to unity.

The macroscopic quantities, such as the electron density n, electron mean energy $\langle U\rangle$, and excitation rate W are the following integrals of the EDF:

$$n(z)=\int_0^\infty U^{1/2}f_0(U+e\varphi(z),z)dU, \quad (5)$$

$$\langle U\rangle(z)=\int_0^\infty U^{3/2}f_0(U+e\varphi(z),z)dU$$
$$\times\left(\int_0^\infty U^{1/2}f_0(U+e\varphi(z),z)dU\right)^{-1}, \quad (6)$$

$$W(z)=N\sqrt{\frac{2}{m_e}}\int_0^\infty U\sum_k Q_k^{\mathrm{in}}(U)f_0(U+e\varphi(z),z)dU. \quad (7)$$

In the present paper, calculations were made for neon at pressures $p=0.5$ and 1.5 Torr (the gas temperature was assumed to be 273 K). The modulation degree of the field was $\alpha=0.9$. At $p=1.5$ Torr the period averaged axial electric field was $E_0=3.25$ V/cm. This is the typical experimental value of the mean axial electric field for a discharge in neon at pressure $p\approx 1.5$ Torr, current $i\approx(10-20)$ mA and tube radius $R_0\approx 1$ cm (see Sec. II). At $p=0.5$ Torr the value $E_0=3$ V/cm was taken. It is also close to the experimental values of the period averaged axial field under these discharge conditions. The kinetic equation was solved for various values of the field spatial period length L in the range $L_S/3$ to L_S ($L_S\approx 5.7$ cm). The step was 0.1 cm($\approx 0.02L_S$) and one or two orders of magnitude smaller in the vicinity of the resonances.

IV. RESONANCE BEHAVIOR OF THE MACROSCOPIC QUANTITIES

In order to illustrate the resonance behavior of the macroscopic quantities, the modulation degrees of the electron density, electron mean energy, and excitation rate (m_n, $m_{\langle U\rangle}$, and m_W, correspondingly) were calculated:

$$m_n=\frac{n_{\max}-n_{\min}}{n_{\max}+n_{\min}}\times 100\,\%, \quad (8)$$

$$m_{\langle U\rangle}=\frac{\langle U\rangle_{\max}-\langle U\rangle_{\min}}{\langle U\rangle_{\max}+\langle U\rangle_{\min}}\times 100\,\%, \quad (9)$$

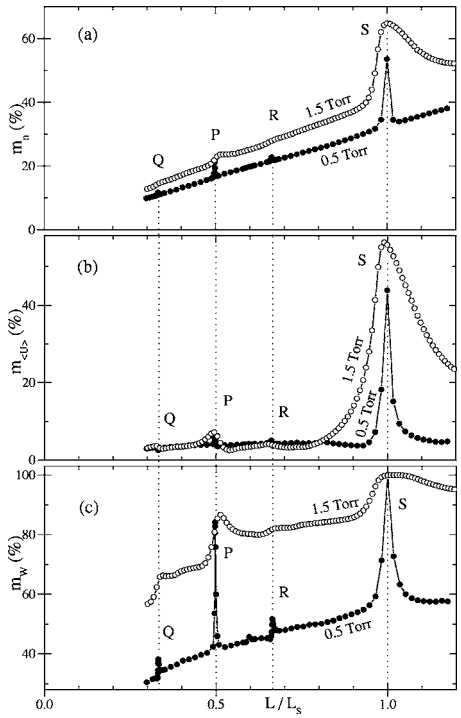

FIG. 2. Calculated dependences of the modulation degrees of the electron density m_n (a), electron mean energy $m_{\langle U\rangle}$ (b), and excitation rate m_W (c) on the reduced spatial period length L/L_S at $p=0.5$ Torr (closed circles) and $p=1.5$ Torr (open circles).

$$m_W = \frac{W_{\max} - W_{\min}}{W_{\max} + W_{\min}} \times 100\,\% . \tag{10}$$

The indices "max" and "min" correspond to the maximum and minimum values of the parameters $n(z)$, $\langle U\rangle(z)$, and $W(z)$ over a spatial period. The modulation degrees $m_n(L)$, $m_{\langle U\rangle}(L)$, and $m_W(L)$ are represented in Figs. 2(a)–2(c) as the functions of the spatial period length L at gas pressures $p=0.5$ and 1.5 Torr. As can be seen from Fig. 2, resonance peaks appear in all the dependences. These peaks are expressed most explicitly in the excitation rate modulation degree $m_W(L)$ [Fig. 2(c)].

At the lower pressure $p=0.5$ Torr the resonance peaks are sharper and narrower than at $p=1.5$ Torr. This effect can be explained qualitatively based on an approximate analysis [6] of the kinetic equation employing an expansion in powers of the small parameter:

$$\varkappa = \frac{6m_e}{M}\left(\frac{U_1}{eE_0\lambda}\right)^2 \approx 3\left(\frac{L_S}{\lambda_\varepsilon}\right)^2, \tag{11}$$

where λ is the electron mean free path with respect to elastic impacts, $\lambda_\varepsilon = \lambda/\sqrt{2m_e/M}$ is the length of electron energy relaxation in elastic collisions. If pressure is decreased three times the parameter $\varkappa$ becomes almost one order of magnitude smaller. Then, as a result of the bunching effect, the EDF is compressed into narrower maxima. This leads to sharper dependences (shown in Fig. 2) in the vicinity of the resonance. The resonances become narrower and more pronounced.

All dependences shown in Fig. 2 have peaks corresponding to the resonances at the values of the spatial period length $L=L_S$, $L_S/2$, and $L_S/3$, which were predicted by linear theory [6,7]. We shall call these resonances S resonance at $L=L_S$, P resonance at $L=L_S/2=L_P$, and Q resonance at $L=L_S/3=L_Q$. S resonance peak corresponds to S striations observed in experiments and has the largest value. P resonance corresponding to P striations is expressed not so explicitly. Self-excited striations corresponding to the weakly expressed Q resonance are not observed in experiments.

In addition to these peaks, a maximum at $L=(2/3)L_S$ is seen in Fig. 2. This resonance is observed distinctly at pressure 0.5 Torr. It was not predicted by linear theory [6,7]. The fall of the potential V_L and the spatial period length L corresponding to this resonance are close to the experimental values of the potential fall V_L and the wavelength L in R striation observed under similar discharge conditions. Experimentally measured values (see Sec. II, Fig. 1) for R striations at $p=1.5$ Torr are $V_L=(12–13)$ V and $L=(3.5–4.0)$ cm. According to calculations, the considered peak (Fig. 2) corresponds to the values $V_L=12.2$ V and $L=3.75$ cm under this pressure. At $p=0.5$ Torr calculations result in $V_L=11.34$ V and $L=3.78$ cm. The resonance at $L=(2/3)L_S=L_R$ will be called an R resonance hereafter.

V. RESONANCE FORMATION OF THE ELECTRON DISTRIBUTION FUNCTION IN THE STRIATIONLIKE FIELDS

Electron distribution functions (EDFs) calculated in the resonance fields with spatial period lengths $L=L_S$, $L_S/2$, and $L_S/3$ (S,P,Q resonances) at $p=0.5$ Torr are given in Figs. 3(a)–3(c). The distance along the axial coordinate z for all three cases is equal to L_S which corresponds to one spatial period for $L=L_S$ (S striation), two spatial periods for $L=L_P=L_S/2$ (P striation), and three spatial periods for $L=L_Q=L_S/3$. The potential drop over this distance is about 17 V, the same for all three cases. As it is seen from Fig. 3, the resonance EDFs have a distinctive structure with maxima which move along the resonance trajectories. The EDFs are compressed to these maxima as a result of the bunching effect. In the case of $L=L_S$ [Fig. 3(a)] the EDF is compressed to one maximum which corresponds to an electron acquiring kinetic energy equal to the excitation threshold U_1 over the distance of one spatial period L_S and successive energy loss in inelastic collisions with atoms. Figure 3(b) shows that in the case of $L=L_P$ the EDF has two maxima which move along two resonance trajectories. Electrons must travel two spatial periods (i.e., the distance $L_S=2L_P$) to attain the kinetic energy equal to U_1. For $L=L_Q$ the picture of electron motion is similar, but there are three maxima in the EDF and three resonance trajectories. Detuning from the resonance values of the spatial period length results in destruction of the regular structure of the EDF [11,12]. Experimental investigations of the EDF in S and P striations [12,14] show a good agreement with the EDFs calculated at $L=L_S$ and $L=L_P$. Striations corresponding to the Q resonance have not been found experimentally.

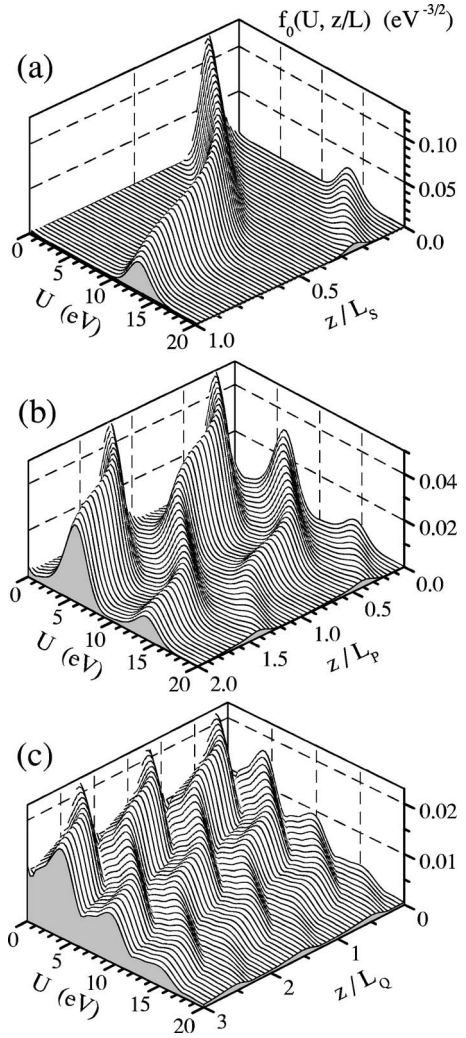

FIG. 3. The EDFs calculated at $p=0.5$ Torr, for the resonances: (a) $L=5.7$ cm$=L_S$, $V_L=17.1$ V, S resonance (S striation); (b) $L=2.834$ cm$=L_P=L_S/2$, $V_L=8.502$ V, P resonance (P striation); and (c) $L=1.89$ cm$=L_Q=L_S/3$, $V_L=5.67$ V, Q resonance. The distance along the coordinate equals L_S in all three cases.

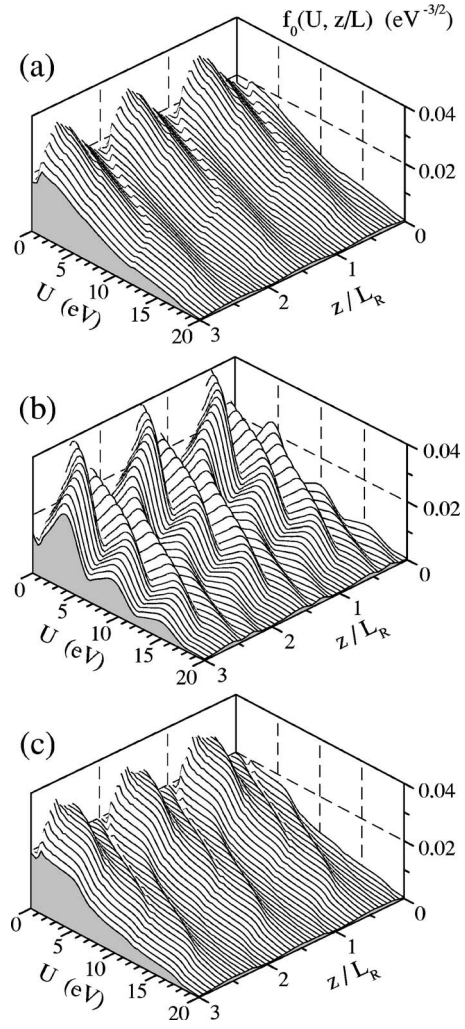

FIG. 4. The EDFs calculated at $p=0.5$ Torr, for (b) R resonance, $L=3.78$ cm$=L_R=(2/3)L_S$ ($V_L=11.34$ V), and in the vicinity of the resonance: (a) $L=3.70$ cm$\approx 0.98L_R$, (c) $L=3.86$ cm$\approx 1.02L_R$.

The EDF resonance formation at $L=L_R=(2/3)L_S$ (R resonance) is illustrated by Fig. 4. The three-dimensional graphs of the EDF calculated at $p=0.5$ Torr for $L=L_R$ and $L=(1\pm 0.02)L_R$ ($\pm 2\%$-detuning) are represented in the figure in variables (kinetic energy, coordinate). As it is shown in Fig. 4(b), the EDF at $L=L_R$ has the regular structure of distinct maxima which move on the plane (energy, coordinate). Small detuning results in destruction of this structure of the EDF [Figs. 4(a) and 4(c)].

If pressure is increased to 1.5 Torr, the EDF maxima become broader and less evident. This can be seen by comparing Figs. 5 and 4(b). As a result, the R resonance presented in Fig. 2 at $p=1.5$ Torr is much weaker than that at $p=0.5$ Torr. Note that S and P striations are observed in experiment in the pressure range $p<(5-7)$ Torr, but R striations at lower pressures only $p<(1.5-2)$ Torr [13], the tube radius $R_0=1$ cm.

The EDF representation in variables (total energy, coordinate) is very informative. In Figs. 6(a)–6(d) these functions are shown at $p=0.5$ Torr for S, P, Q, and R resonances. The distance along the coordinate z for all four cases is equal to $2L_S$ which corresponds to the two spatial periods at $L=L_S$, four periods at $L=L_P=L_S/2$, six periods at $L=L_Q=L_S/3$, and three periods at $L=L_R=(2/3)L_S$. The total energy range for all four graphs is the doubled fall of the potential on the S

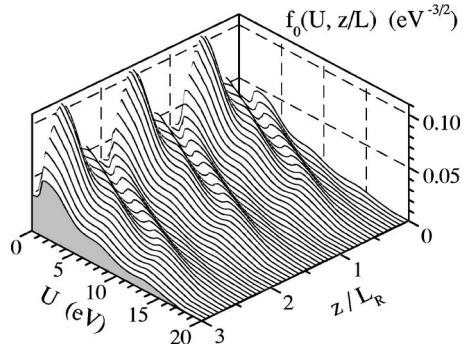

FIG. 5. The EDF calculated at $p=1.5$ Torr, for R resonance: $L=3.75$ cm$=L_R=(2/3)L_S$, $V_L=12.2$ V.

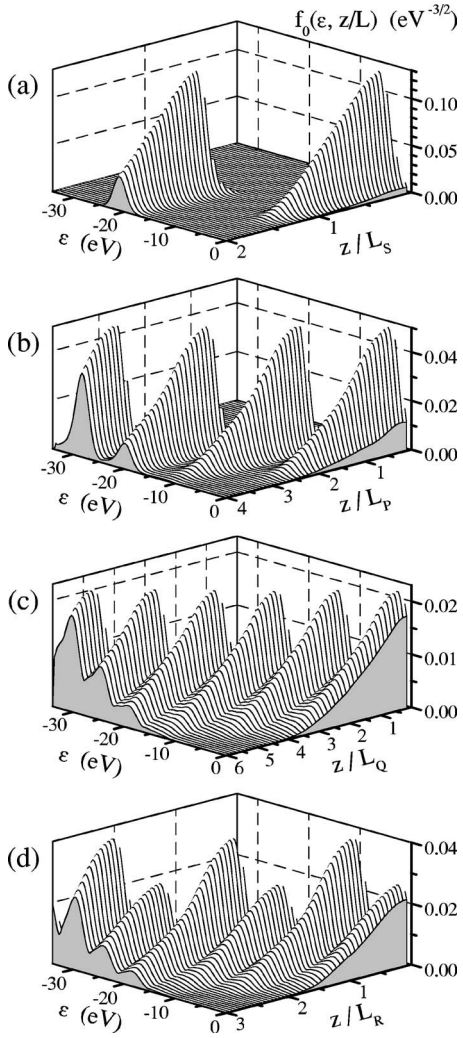

FIG. 6. The EDFs in variables (total energy, coordinate) calculated at $p=0.5$ Torr, for S (a), P (b), Q (c), and R (d) resonances. The distance along the coordinate equals $2L_S$ in all four cases. The graphs correspond to Figs. 3 and 4(b).

striation length $2E_0L_S=2V_L^{(S)}$ which slightly exceeds two excitation thresholds ($\approx$35 eV).

There is a principal difference between the distribution functions at $L=L_R$ [Fig. 6(d)] and $L=L_S,L_P,L_Q$ [Figs. 6(a)–6(c)]. For an R resonance the maxima in the EDF $f_0(\varepsilon,z)$ have different amplitudes. For S, P, and Q resonances all maxima are of the same amplitude. This follows from the fact that in the case of $L=L_R$ one spatial period length L_R contains two maxima of the function $f_0(U,z)|_{U=\text{const}}$ [see Fig. 4(b)] and in other cases one spatial period length $L=L_S,L_P,L_Q$ contains one maximum of the function $f_0(U,z)|_{U=\text{const}}$ (see Fig. 3).

The EDF maxima move in the plane (ε,z), along the resonance trajectories. For Q and R resonances there are three resonance trajectories since in both cases the function $f_0(\varepsilon,z)|_{z=\text{const}}$ has three maxima [Figs. 3(c), 4(b), 6(c), and 6(d)]. However, the picture of the resonance trajectories is different in these two cases.

In Figs. 7(a)–7(d) the qualitative picture of the EDF maxima displacements along the resonance trajectories is

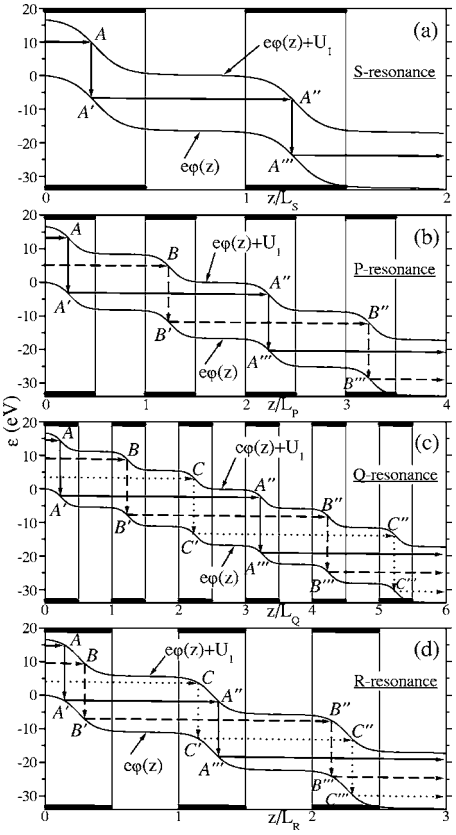

FIG. 7. The picture of the resonance trajectories for the cases: (a) $L=L_S$, S resonance; (b) $L=L_P=L_S/2$, P resonance; (c) $L=L_Q=L_S/3$, Q resonance; (d) $L=L_R=(2/3)L_S$, R resonance. The distance along the coordinate equals $2L_S$ in all four cases.

represented in the plane (total energy, coordinate) for various resonances. The curves $\varepsilon=e\varphi(z)$ and $\varepsilon=e\varphi(z)+U_1$ where the electron kinetic energy is equal to 0 or U_1, correspondingly, are shown. The regions of strong field [regions of an abrupt fall of $e\varphi(z)$] are marked in Fig. 7 by thick parts of the z axis. The electric field profile $E(z)$ chosen here for better visualization is modulated sharper than the sinusoidal function. It is seen from Figs. 7(a)–7(c) that there are one (A), two (A,B), or three (A,B,C), resonance trajectories for S, P, and Q resonances, respectively. The jumps AA', $A''A'''$, BB', $B''B'''$, CC', $C''C'''$ (indicating the electron energy loss in inelastic collisions) take place in the strong field regions. One jump occurs in each strong field region. The distances $A'A''$, $B'B''$, $C'C''$ are equal to L_S for all three cases [Figs. 7(a)–7(c)].

Figure 7(d) shows that there are three resonance trajectories for an R resonance, as was already mentioned above. Nevertheless, the structure of the trajectories is more complicated than it was for a Q resonance. In each strong field region two jumps (AA' and BB', CC' and $A''A'''$, $B''B'''$ and $C''C'''$) occur. It is connected with the presence of two EDF maxima in one spatial period length L_R, as was mentioned above. The configuration of the curves $\varepsilon=e\varphi(z)$ and $\varepsilon=e\varphi(z)+U_1$ in the case of the electric field with the spatial period being equal to L_R is such that the distances $A'A''$ and $B'B''$ (indicating electron acceleration to the kinetic energy

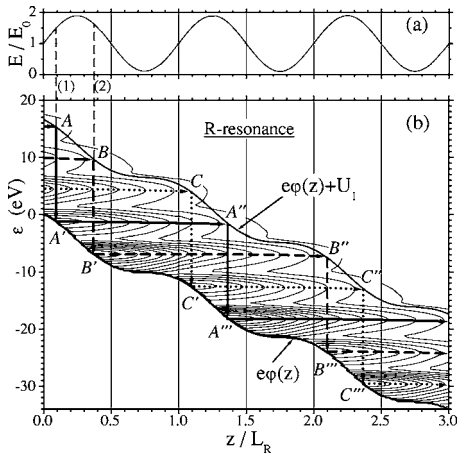

FIG. 8. Contour graph of the EDF calculated at $p=0.5$ Torr, for R resonance: $L=L_R=(2/3)L_S=3.78$ cm, $V_L=11.34$ V in the plane (total energy, coordinate) (b). The graph is correlated with the electric field (a). Resonance trajectories are shown with arrows.

U_1) are different. Therefore electrons can acquire energy U_1 over a distance either slightly exceeding L_R or almost equal $2L_R$, as shown by the arrows $A'A''$ and $B'B''$ in Fig. 7(d). The picture of the resonance trajectories in this case is reproduced completely after the distance $2L_S=3L_R$.

Figures 7(a)–7(d) give the schemes of the resonance trajectories. In Fig. 8(b) the contour graph of the EDF in variables (total energy, coordinate) calculated at $p=0.5$ Torr for an R resonance is represented. The graph is correlated with the electric field [Fig. 8(a)]. The resonance trajectories (displacements of the EDF maxima) are shown by arrows. One can see that the picture is similar to that shown in Fig. 7(d). According to Fig. 8(b), the maximum of smaller amplitude is formed at the point (1) ($z\approx 0.1L_R$), and that of larger amplitude appears at the point (2) ($z\approx 0.4L_R$). The smaller maximum moves along the line $\varepsilon\approx$const from $z\approx 0.1L_R$ to $z\approx 1.4L_R$ [Fig. 8(b), arrow $A'A''$]. Over this distance (slightly exceeding L_R) electrons attain kinetic energy equal to the excitation threshold U_1. Then the jump $A''A'''$ takes place (the energy U_1 is lost in inelastic collision). The larger maximum starts from the point (2) ($z\approx 0.4L_R$) and acquires the kinetic energy equal to U_1 at the point $z\approx 2.1L_R$ [Fig. 8(b), arrow $B'B''$]. Then the loss of energy in inelastic impact ($B''B'''$) occurs. The smaller maximum gains kinetic energy equal to the excitation threshold, over a length slightly exceeding L_R, and the larger maximum acquires the same energy on the length about $2L_R$. Transitions from the smaller maximum to the larger one and vice versa take place during the jumps. Therefore, electrons, twice in the distance $3L_R$, acquire and lose in inelastic collisions energy equal to the excitation threshold. It results in formation of the EDF with spatial period $L_R=(2/3)L_S$.

The difference in the maximum amplitudes is connected with the fact that the smaller maximum starts from the point (1) ($z\approx 0.1L_R$) where the field $E(z)$ increases, and the larger maximum starts from the point (2) ($z\approx 0.4L_R$) where $E(z)$ decreases. The magnitudes of $E(z)$ at $z\approx 0.1L_R-0.4L_R$ are larger than those at $z\approx 0.4L_R-0.7L_R$. It results in stronger acceleration of electrons moving from the point (1) along $A'A''$ compared with electron acceleration from the point (2) along $B'B''$. As a result, the EDF maxima of different amplitudes are formed.

Thus, similarly to S and P striations, it is possible to interpret R striations as a resonance phenomenon in spatially periodic electric fields with spatial period length $L=(2/3)L_S$. Such resonances are well-known in nonlinear dynamics [17].

VI. NONLINEAR BEHAVIOR OF THE ELECTRONS MOTION

Behavior of the electrons motion in the resonant electric field was described in Sec. I. From this description it is clear that there exists a characteristic inner spatial period L_S defined by gas type and by discharge conditions so that in the electric field with spatial period L_S the properties of electrons (the form of the EDF) are periodically repeated. In the case when the spatial period of the electric field (external period L) is detuned from this inner period, the properties of electrons may not be repeated. The task can be formulated as follows: for a given internal period L_S find all values of external period L which deliver periodicity of electron properties.

Let z_n be a spatial position of electron with the kinetic energy U and the total energy ε_n:

$$z_n=-\frac{\varepsilon_n-U}{e_0E_0}+\frac{\alpha L}{2\pi}\cos\frac{2\pi z_n}{L}. \tag{12}$$

The next position of electron with the same kinetic energy can be written as

$$z_{n+1}=-\frac{\varepsilon_{n+1}-U}{e_0E_0}+\frac{\alpha L}{2\pi}\cos\frac{2\pi z_{n+1}}{L}. \tag{13}$$

Using the fact that $\varepsilon_{n+1}=\varepsilon_n-e_0V_L^{(S)}$, Eq. (13) can be rewritten as

$$\begin{aligned} z_{n+1}&=-\frac{\varepsilon_n-U}{e_0E_0}+\frac{V_L^{(S)}}{E_0}+\frac{\alpha L}{2\pi}\cos\frac{2\pi z_{n+1}}{L}\\ &=z_n+L_S+\frac{\alpha L}{2\pi}\left(\cos\frac{2\pi z_{n+1}}{L}-\cos\frac{2\pi z_n}{L}\right). \end{aligned} \tag{14}$$

Dividing the last equation over spatial period L of the electric field we obtain

$$\Theta_{n+1}=\Theta_n+\Omega+\frac{\alpha}{2\pi}[\cos(2\pi\Theta_{n+1})-\cos(2\pi\Theta_n)], \tag{15}$$

where $\Theta_n=z_n/L \bmod 1$ is the phase position within a single period of L, $\Omega=L_S/L$ is the ratio of inner and outer periods. In order to produce a map let us introduce the function $A(\Theta)$:

$$A(\Theta_n)=\Theta_{n+1}-\Theta_n=\Omega+\frac{\alpha}{2\pi}[\cos(2\pi\Theta_{n+1})-\cos(2\pi\Theta_n)]. \tag{16}$$

After some manipulation we get

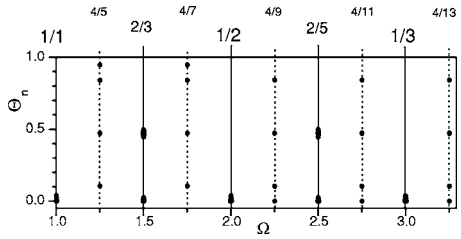

FIG. 9. Histogram of trajectories for map (18) at different Ω. Spots show positions where more than 25% of sequential values Θ_n are concentrated. The sum over spots lying along vertical lines gives 100% of points.

$$A(\Theta_n) = \Omega - \frac{\alpha}{2\pi}\cos(2\pi\Theta_n)\{1 - \cos[2\pi A(\Theta_n)] + \tan(2\pi\Theta_n)\sin[2\pi A(\Theta_n)]\}. \quad (17)$$

The expression (17) represents an implicit equation for $A(\Theta_n)$. $A(\Theta_n)$ is a periodic bounded function of Θ_n as can be seen from Fig. 7. The function A is a distance in "horizontal" direction between curves $e\varphi(z)$ and $e\varphi(z)+U_1$. The map can be written as follows:

$$\Theta_{n+1} = \Theta_n + A(\Theta_n). \quad (18)$$

This expression describes a nonlinear map, similar to the circle map in [17]. This map indicates the reason for nonlinearity: the motion of electrons in normal space is mapped nonlinearly onto energy space. The map (18) can be investigated for periodic solutions. For some starting value Θ_0 a series of Θ_n can be calculated. In the case of periodicity a set of possible Θ_n values should be limited by a small integer amount of values: 1, 2, 3, or 4 which correspond to the periodicity or period-2, period-3, or period-4 quasiperiodicity, respectively. Once calculated a series Θ_n for given Ω can be used for building a histogram of Θ_n values. The number of maxima in the histogram can help judge the periodicity.

Figure 9 shows a contour plot for a set of histograms of Θ_n series for different values of Ω. One can see in this figure the values of Θ where more than 25% of points Θ_n series are concentrated. The sum over Θ for a given value of Ω gives 100% of points Θ_n. One can clearly see that for some values of Ω we obtain cycling values of Θ: for $\Omega=1,2,3$ it is only $\Theta=0$, for $\Omega=1.5,2.5$ it is $\Theta=0$ and 0.5, for $\Omega=1.25,1.75$ it is $\Theta=0.1,0.47,0.85,0.93$, and so on. These values of Ω correspond to the L/L_S ratios shown on the top of Fig. 9. The ratios are given by a so-called Farey tree—a characteristic of a circle map [17]. The investigated map gives resonances at fractions of L_S: 1/3 (Q resonance), 1/2 (P resonance), 2/3 (R resonance), and 1 (S resonance). The latter three fractions correspond to waves which can be observed experimentally. In the case of periodicity of map (18) synchronization of the microscopic kinetic motion of electrons with the macroscopically defined electric field takes place.

S, P, and R striations can exist in self-excited mode. After applying an external periodic disturbance to the positive column other periodic states can also be revealed [18] which correspond to the resonances 1/3 and 2/5 of the Farey tree. These waves do not exist in self-excited mode as they are effectively damped.

When the gas pressure is increased the resonances disappear due to the increasing role of elastic collisions. The electron energy balance is then no longer controlled by inelastic impacts.

VII. INFLUENCE OF INELASTIC COLLISIONS ON THE RESONANCE BEHAVIOR OF THE EDF

It is interesting to analyze the dependence of the EDF resonance formation on the magnitude of the inelastic electron-atom collision frequency. There are two factors leading to compression of the EDF to the resonance maxima (the bunching effect): the small fraction of electron energy losses in elastic collisions and the presence of several excited states of atomic neon [6,9,10]. Since low pressures ($\approx$0.5 Torr) are under consideration, the second factor plays a significant role.

Analytical theory of the EDF formation in the spatially periodic fields usually employs the "black wall" approximation corresponding to infinitely large flux of electrons into the inelastic region at $U>U_1$. This limiting case can be modeled numerically by increasing formally the values of all inelastic collision cross sections Q_k^{in}. It results in stronger decrease of the EDF in the region $U>U_1$. In the present paper the EDF and macroscopic quantities were calculated in the vicinity of the resonance not only for realistic values of Q_k^{in} but also for ten times increased values of Q_k^{in}.

The calculation results for the modulation degrees of the electron density, electron mean energy, and excitation rate at $p=0.5$ Torr are presented in Figs. 10(a)–10(c) for realistic and ten times increased cross sections. According to Fig. 10 if the cross-section magnitudes Q_k^{in} are increased, the resonances become sharper and the resonance peaks significantly larger.

The regular structure of the EDF becomes more pronounced, with the EDF maxima being narrower. As an example of the influence of the inelastic impact intensity on the resonance EDF formation, the three-dimensional graphs of the EDF for an R resonance at $p=0.5$ Torr are shown in Figs. 11(a)–11(c) for the ten times increased, actual, and ten times decreased cross sections Q_k^{in}. In Fig. 11(a) the EDF maxima are significantly narrower than those in Fig. 11(b). In Fig. 11(c) the EDF structure is completely destroyed. The spatially periodic solution of the kinetic equation with increased Q_k^{in} can be attained over a few times longer distance than it is established in the case of the actual cross-section values.

VIII. CONCLUSION

In the present paper, resonance formation of the EDF in sinusoidally modulated striationlike fields in inert gases at low pressures and small currents was analyzed on the basis of an accurate numerical solution of the Boltzmann kinetic equation. Dependences of the degrees of modulation of the macroscopic quantities (electron density, electron mean energy, and excitation rate) on the spatial period length L of the sinusoidaly modulated electric field are shown to have an

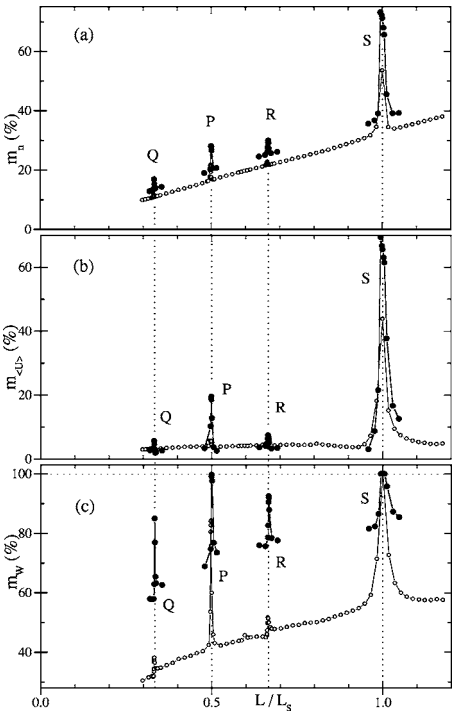

FIG. 10. Dependences of the modulation degrees of the electron density m_n (a), electron mean energy $m_{\langle U\rangle}$ (b), and excitation rate m_W (c) on the reduced spatial period length L/L_S at $p=0.5$ Torr, calculated for the 10 times increased inelastic collisions cross sections Q_k^{in} (closed circles) and for the real values of Q_k^{in} (open circles).

explicitly resonance character. The resonances become sharper with decreasing pressure. In addition to resonances at $L=L_S$ (S resonance), $L_S/2$ (P resonance), and $L_S/3$ (Q resonance) predicted by linear theory, the calculations indicate the presence of a resonance at $L=(2/3)L_S$ which is better expressed at lower pressures. Such resonances are well-known in nonlinear dynamics. It is possible to correlate this resonance to the R striation observed in experiment, similarly to S and P striations which correspond to the resonances at $L=L_S$ and $L=L_S/2$.

If the field spatial period length L has the resonance value, a regular structure is formed in the EDF with maxima moving in the plane (energy, coordinate) along the resonance trajectories. A small detuning from the resonance length results in destruction of this structure. In the S striation case ($L=L_S$) the EDF is compressed to one maximum which moves along the resonance trajectory. In the case of a P striation ($L=L_S/2$) there are two maxima in the EDF and two resonance trajectories. In the case of $L=(2/3)L_S$ the EDF structure is more complicated than in S and P striations. There are three maxima in the EDF and three resonance trajectories. In addition, one spatial period length L contains not

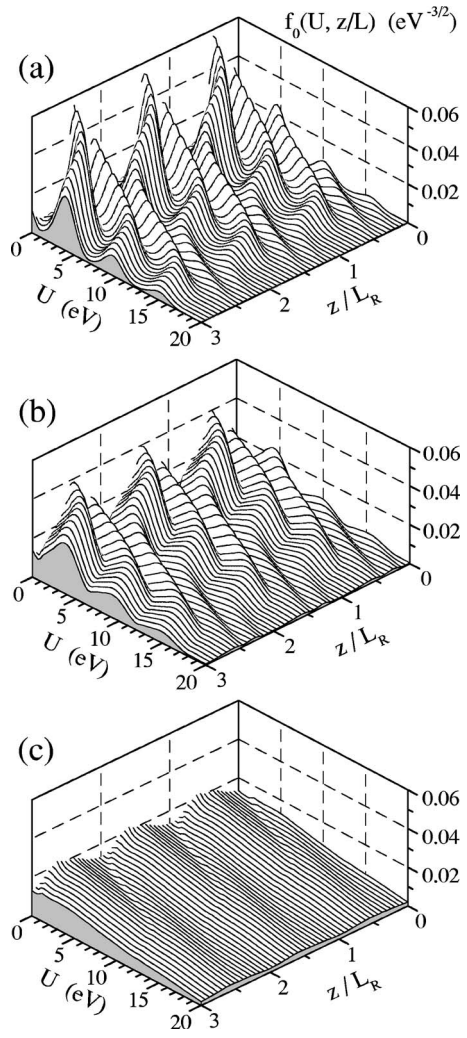

FIG. 11. The EDFs calculated for the 10 times increased inelastic collisions cross sections Q_k^{in} (a), for the real values of Q_k^{in} (b), and for the 10 times decreased Q_k^{in} (c). $p=0.5$ Torr, $L=(2/3)L_S$, R resonance.

one (as at $L=L_S$, $L_S/2$, $L_S/3$) but two EDF maxima of different amplitude.

In the present paper, the influence of inelastic collisions on the EDF formation was also considered. The resonances are shown to become sharper at low pressures with formally increased magnitudes of the inelastic electron-atom collision cross sections. It is connected with the significant influence of the presence of several excited atomic states on the electron bunching effect.

ACKNOWLEDGMENT

The work was supported by Grant No. E02-3.2-93 of the Ministry of Education of Russian Federation.

[1] L. Pekarek, Sov. Phys. Usp. **11**, 188 (1968).
[2] A. V. Nedospasov, Sov. Phys. Usp. **11**, 174 (1968).
[3] N. L. Oleson and A. W. Cooper, Adv. Electron. Electron Phys. **24**, 155 (1968).
[4] Y. P. Raizer, *Gas Discharge Physics* (Springer-Verlag, Berlin, 1997).
[5] T. Ruzicka and K. Rohlena, Czech. J. Phys., Sect. B **22**, 906 (1972).
[6] L. D. Tsendin, Sov. J. Plasma Phys. **8**, 228 (1982).
[7] L. D. Tsendin, Zh. Tekh. Fiz. **52**, 635 (1982); **52**, 643 (1982).
[8] F. Sigeneger and R. Winkler, Contrib. Plasma Phys. **36**, 551 (1996).
[9] F. Sigeneger, Y. B. Golubovskii, I. A. Porokhova, and R. Winkler, Plasma Chem. Plasma Process. **18**, 153 (1998).
[10] Y. B. Golubovskii, I. A. Porokhova, J. Behnke, and V. O. Nekutchaev, J. Phys. D **31**, 2447 (1998).
[11] F. Sigeneger and R. Winkler, Plasma Chem. Plasma Process. **20**, 429 (2000).
[12] Y. B. Golubovskii, R. V. Kozakov, J. Behnke, C. Wilke, and V. O. Nekutchaev, Phys. Rev. E **68**, 026404 (2003).
[13] A. Rutscher, Habilitation, Greifswald University, Greifswald, 1964).
[14] Y. B. Golubovskii, V. O. Nekutchaev, N. S. Ponomarev, and I. A. Porokhova, Tech. Phys. **42**, 997 (1997).
[15] Y. B. Golubovskii, R. V. Kozakov, V. A. Maiorov, J. Behnke, and J. F. Behnke, Phys. Rev. E **62**, 2707 (2000).
[16] Y. B. Golubovskii, V. A. Maiorov, I. A. Porokhova, and J. Behnke, J. Phys. D **32**, 1391 (1999).
[17] H. G. Schuster, *Deterministic Chaos: An Introduction* (VCH, Weinheim, 1989).
[18] B. Albrecht, H. Deutsch, R. W. Leven, and C. Wilke, Phys. Scr. **47**, 196 (1993).